Molecular-Orbital Studies of Charge-Carrier Transport in Orthorhombic Sulfur. I. Molecular Orbitals of S_8

Inan Chen
Research Laboratories, Xerox Corporation, Rochester, New York 14603
(Received 16 January 1970)

Stimulated by the interesting transport experiments on orthorhombic sulfur by Spear and co-workers, we have carried out a semiempirical molecular-orbital calculation of the S_8 molecule, the building block of the molecular crystal. The molecular orbitals are constructed from linear combinations of atomic $3s$, $3p$ orbitals according to the irreducible representations of the molecular symmetry group. It is found that because of the nonplanar (puckered ring) geometry of the molecule, the mixing of σ and lone-pair hybrids in the molecular orbitals is not negligible. The molecular energy-level scheme predicts a set of electronic transitions which can be compared, with certain reservations, to the absorption spectrum of sulfur in hexane. It also predicts two forbidden transitions at 2–3 eV which could be responsible for the yellow color of the crystal. The sensitivities of the molecular orbitals and energies with respect to the variation in the parameter of the calculation are discussed. It is concluded that the results are satisfactory for use as the starting point in the studies of the crystal states, which is carried out in the following paper.

I. INTRODUCTION

The electric and optical properties of orthorhombic sulfur have recently been studied in detail by Spear and co-workers.[1] Of particular interest is the different behavior of the electron and the hole-transport parameters in this molecular crystal. According to them, an excess electron propagates by an intermolecular-hopping process while a hole moves through the lattice in a narrow polaron band. This is qualitatively accounted for by noting that the electron band is formed from the σ^* orbitals while the hole band is generated by the more overlapping π^* (lone-pair) orbitals.

In contrast to the extensive theoretical studies on the electronic states of organic molecular crystals,[2] there is no such work on orthorhombic sulfur, nor on the S_8 molecule, which is the building block of the molecular crystal, except for the unpublished work of Gibbons. Gibbons has analyzed the molecular orbitals (MO) in terms of the σ and π orbitals.[3] He has neglected the mixing between these two types of orbitals which, as shown in Sec. VII, is not negligible because the molecule is not planar. No effect of molecular symmetry was considered in his analysis. The lack of theoretical work on the S_8 molecule is probably due to the difficulty in obtaining a molecular electronic spectrum. Sulfur dissolves considerably only in CS_2 whose absorption masks those of the solute. To the best of the author's knowledge, only a broad, not very well-resolved spectrum of sulfur in hexane has been published.[4]

In this paper we carry out a semiempirical calculation[5] of the MO of the S_8 molecule. Our major purpose is not the identification of the molecular spectrum but the interpretation of the different behavior of electron- and hole-transport parameters in orthorhombic sulfur crystals.

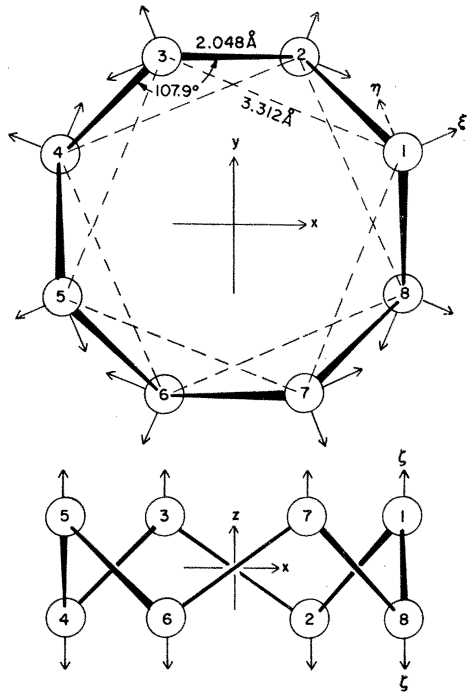

FIG. 1. Structure of S_8 molecule. Top: viewed perpendicular to the molecular planes. Bottom: viewed parallel to the molecular planes. The atomic coordinates (ξ_i, η_i, ζ_i) defined in Sec. II and the molecular coordinates (x, y, z) defined in Sec. III are also shown.

The structure of the S_8 molecule is a puckered ring (Fig. 1).[6] Each atom has two nearest neighbors at a distance of 2.048 Å and an average bond angle of 107.9°. The odd-numbered atoms are located at the corners of a square, 3.312 Å on one side. The even-numbered atoms are located at the corners of another square of the same size but rotated by 45° with respect to the former. The two planes of the squares are parallel and are separated by 0.991 Å.

II. HYBRIDIZATION OF ATOMIC ORBITALS

The valence-electron orbitals 3*s* and 3*p* are hybridized into two directed-bond (σ) hybrids a and b pointing toward the two nearest neighbors, respectively, and two equivalent lone-pair hybrids c and d:

$$a = \alpha s + (1-\alpha^2)^{1/2} p_a \ , \tag{1}$$

$$b = \alpha s + (1-\alpha^2)^{1/2} p_b \ , \tag{2}$$

$$c = (0.5-\alpha^2)^{1/2} s + (0.5+\alpha^2)^{1/2} p_c \ , \tag{3}$$

$$d = (0.5-\alpha^2)^{1/2} s + (0.5+\alpha^2)^{1/2} p_d \ , \tag{4}$$

where p_a and p_b are linear combinations of p_x, p_y, and p_z pointing towards the two nearest neighbors, respectively, and p_c and p_d are similar combinations which can be determined by orthonormality requirements. The hybridization constant α is determined from the bond angle θ and the orthogonality of a and b as

$$\alpha = [-\cos\theta/(1-\cos\theta)]^{1/2} \ , \tag{5}$$

which has the value of 0.4849 with the θ value given above.

We shall define a set of right-handed coordinate systems (ξ_i, η_i, ζ_i) at atom i such that the ξ_i axis lies on the direction connecting the center of the square and the atom, pointing outward; and the ζ_i axis is perpendicular to the plane of the square and pointing away from the other square (Fig. 1). In this coordinate system (say, of atom 1), the two nearest neighbors (2 and 8) are located at $[-\frac{1}{2}L \times(\sqrt{2}-1), \pm\frac{1}{2}L, -H]$, where L is the side length of the square and H is the separation between the two squares. Thus the combinations p_a and p_b in Eqs. (1) and (2) can be written as

$$p_{a,b} = \beta_1 \xi_i \pm \beta_2 \eta_i + \beta_3 \zeta_i \ , \tag{6}$$

with

$$\beta_1 = -L(\sqrt{2}-1)/2B \ , \tag{7}$$

$$\beta_2 = L/2B \ , \tag{8}$$

$$\beta_3 = -H/B \ , \tag{9}$$

where B is the bond length.

Now if the p-orbital combinations for the lone pairs, Eqs. (3) and (4), are written as

$$p = \gamma_1 \xi_i + \gamma_2 \eta_i + \gamma_3 \zeta_i \ , \tag{10}$$

then, from the orthogonality relations, we have

$$\alpha(0.5-\alpha^2)^{1/2} + [(1-\alpha^2)(0.5+\alpha^2)]^{1/2} \times(\beta_1\gamma_1 \pm \beta_2\gamma_2 + \beta_3\gamma_3) = 0 \ , \tag{11}$$

which immediately gives

$$\gamma_2 = 0, \tag{12}$$

$$\beta_1\gamma_1 + \beta_3\gamma_3 = -\alpha[(0.5-\alpha^2)/(1-\alpha^2)(0.5+\alpha^2)]^{1/2}. \tag{13}$$

Combining with the normalization requirement,

$$\gamma_1^2 + \gamma_3^2 = 1 \ . \tag{14}$$

Equation (13) gives two sets of solutions for γ_1 and γ_3.

Using the geometrical data given above, and Eqs. (5)–(14), the hybridization of S atoms in S_8 molecules are found to be

$$a_i = 0.4849 s_i - 0.2929 \xi_i + 0.7071 \eta_i - 0.4232 \zeta_i \ , \tag{15}$$

$$b_i = 0.4849 s_i - 0.2929 \xi_i - 0.7071 \eta_i - 0.4232 \zeta_i \ , \tag{16}$$

$$c_i = 0.5147 s_i + 0.8574 \xi_i \ , \tag{17}$$

$$d_i = 0.5147 s_i - 0.3055 \xi_i + 0.8011 \zeta_i \ . \tag{18}$$

The MO's are formed from linear combinations of these hybrids of each atom according to the molecular symmetry.

III. MOLECULAR SYMMETRY AND LINEAR COMBINATIONS OF HYBRID ORBITALS

The symmetry group of the ring molecule is D_{4d}. The 16 symmetry operations are: two eightfold rotation reflections ($\hat{S}_8$), two fourfold rotations $(\hat{S}_8)^2$, two 135° rotation reflections $(\hat{S}_8)^3$, one twofold rotation $(\hat{S}_8)^4$, four twofold rotations (C_{2x}) perpendicular to the previous diad axis, four mirror planes (σ_d), and the identity. There are four one-dimensional and three two-dimensional irreducible representations. The character table is given in Herzberg's book.[7]

We shall define molecular coordinates (x, y, z) with the origin at the center of molecule (Fig. 1). The z axis coincides with the rotation-reflection axis, and the x axis coincides with one of the twofold axes (C_{2x}) bisecting the 1-8 bond. The other three C_{2x} axes bisect the 1-2, 2-3, and 3-4 bonds. The mirror planes are those perpendicular to the molecular plane (x-y plane), including the z axis, and passing through the atoms 1, 2, 3, and 4, respectively.

The hybrids a_i and b_i (i = 1-8) transform among

themselves under the symmetry operations, whereas the hybrids c_i and d_i transform into the same type of hybrids only. Linear combinations of hybrid orbitals (LCHO) which transform according to the irreducible representations of the symmetry group can be found by the well-known technique.[8] The results are given in Table I.

IV. OVERLAP AND GROUP OVERLAP INTEGRALS

For the normalization of the LCHO's of Table I and the ultimate determination of the MO's, we need to calculate the overlap integrals between two hybrid orbitals centered at different atoms, and the

TABLE I. Linear combinations of hybrid orbitals according to the irreducible representations of D_{4d}. The Σ is over the index i from 1 to 8. The normalization factor N, Eq. (21), is given in the last column.

Ir. Rep.	LCHO	N
A_1	$\phi_1=\Sigma\,(a_i+b_i)$	0.186 6
	$\phi_2=\Sigma\,c_i$	0.319 1
	$\phi_3=\Sigma\,d_i$	0.376 0
A_2	$\phi_1=\Sigma\,(-1)^{i+1}\,(a_i-b_i)$	0.370 1
B_1	$\phi_1=\Sigma\,(a_i-b_i)$	0.224 7
B_2	$\phi_1=\Sigma\,(-1)^{i+1}\,(a_i+b_i)$	0.362 5
	$\phi_2=\Sigma\,(-1)^{i+1}\,c_i$	0.385 9
	$\phi_3=\Sigma\,(-1)^{i+1}\,d_i$	0.306 8
$E_{1(x)}$	$\phi_1=\sqrt{2}\,(a_1-a_4-a_5+a_8)+(b_1+b_2-b_3-b_4-b_5-b_6+b_7+b_8)$	0.252 0
	$\phi_2=\sqrt{2}\,(a_2-a_3-a_6+a_7)+(b_1-b_2+b_3-b_4-b_5+b_6-b_7+b_8)$	0.227 7
	$\phi_3=(\sqrt{2}+1)\,(c_1-c_4-c_5+c_8)+(c_2-c_3-c_6+c_7)$	0.179 4
	$\phi_4=(\sqrt{2}+1)\,(d_1-d_4-d_5+d_8)+(d_2-d_3-d_6+d_7)$	0.208 4
$E_{1(y)}$	$\phi_1=\sqrt{2}\,(a_2+a_3-a_6-a_7)+(b_1+b_2+b_3+b_4-b_5-b_6-b_7-b_8)$	0.252 0
	$\phi_2=\sqrt{2}\,(a_1+a_4-a_5-a_8)+(-b_1+b_2+b_3-b_4+b_5-b_6-b_7+b_8)$	0.227 7
	$\phi_3=(c_1+c_4-c_5-c_8)+(\sqrt{2}+1)\,(c_2+c_3-c_6-c_7)$	0.179 4
	$\phi_4=(d_1+d_4-d_5-d_8)+(\sqrt{2}+1)\,(d_2+d_3-d_6-d_7)$	0.208 4
$E_{2(x^2-y^2)}$	$\phi_1=a_1-a_2-a_3+a_4+a_5-a_6-a_7+a_8$	0.550 7
	$\phi_2=b_1-b_2-b_3+b_4+b_5-b_6-b_7+b_8$	0.279 1
	$\phi_3=c_1-c_2-c_3+c_4+c_5-c_6-c_7+c_8$	0.359 6
	$\phi_4=d_1-d_2-d_3+d_4+d_5-d_6-d_7+d_8$	0.374 0
$E_{2(xy)}$	$\phi_1=b_1+b_2-b_3-b_4+b_5+b_6-b_7-b_8$	0.550 7
	$\phi_2=a_1+a_2-a_3-a_4+a_5+a_6-a_7-a_8$	0.279 1
	$\phi_3=c_1+c_2-c_3-c_4+c_5+c_6-c_7-c_8$	0.359 6
	$\phi_4=d_1+d_2-d_3-d_4+d_5+d_6-d_7-d_8$	0.374 0
$E_{3(yz)}$	$\phi_1=\sqrt{2}\,(a_1-a_4-a_5+a_8)+(-b_1-b_2+b_3+b_4+b_5+b_6-b_7-b_8)$	0.257 2
	$\phi_2=\sqrt{2}\,(a_2-a_5-a_6+a_7)+(-b_1+b_2-b_3+b_4+b_5-b_6+b_7-b_8)$	0.268 8
	$\phi_3=(\sqrt{2}-1)\,(c_1-c_4-c_5+c_8)+(-c_2+c_3+c_6-c_7)$	0.497 3
	$\phi_4=(\sqrt{2}-1)\,(d_1-d_4-d_5+d_8)+(-d_2+d_3+d_6-d_7)$	0.429 5
$E_{3(xz)}$	$\phi_1=\sqrt{2}\,(-a_2-a_3+a_6+a_7)+(b_1+b_2+b_3+b_4-b_5-b_6-b_7-b_8)$	0.257 2
	$\phi_2=\sqrt{2}\,(-a_1-a_4+a_5+a_8)+(-b_1+b_2+b_3-b_4+b_5-b_6-b_7+b_8)$	0.268 8
	$\phi_3=(\sqrt{2}-1)\,(-c_2-c_3+c_6+c_7)+(c_1+c_4-c_5-c_8)$	0.497 3
	$\phi_4=(\sqrt{2}-1)\,(-d_2-d_3+d_6+d_7)+(d_1+d_4-d_5-d_8)$	0.429 5

group overlap integrals between two LCHO's of the same irreducible representations.

A LCHO is represented by

$$\phi_k = N_k \sum_i f_{ki} h_i \ , \tag{19}$$

where h_i represents a hybrid orbital, f_{ki} is a constant coefficient, and N_k is the normalization factor. The latter is related to the overlap integrals,

$$S_{ij} = \langle h_i | h_j \rangle \ , \tag{20}$$

by $$N_k^2 \sum_i \sum_j f_{ki} f_{kj} S_{ij} = 1 \ . \tag{21}$$

Since the hybrid orbital h_i is given in terms of atomic orbitals U_μ by

$$h_i = \sum_\mu \alpha_{i\mu} U_\mu \ , \tag{22}$$

the overlap integral S_{ij} can be written as

$$S_{ij} = \sum_\mu \sum_\nu \alpha_{i\mu} \alpha_{j\nu} S_{\mu\nu} \ , \tag{23}$$

where the coefficients $\alpha_{i\mu}$ are those given in Eqs. (15)–(18), and the overlap integrals $S_{\mu\nu}$ between two atomic orbitals can be calculated by the method of Mulliken, Rieke, Orloff, and Orloff.[9] We have calculated the overlap integrals using the analytic Hartree-Fock wave functions of Watson and Freeman.[10] The four basic overlap integrals for the nearest-neighbor and the next-nearest-neighbor distances are given in Table II. The overlap integral $S_{\mu\nu}$ is then obtained from these basic integrals by decomposing each orbital U_μ and U_ν into the σ and π components. The matrix $(S_{\mu\nu})$ is, in fact, 32×32 in dimension. However, because of the symmetry, it breaks down into 4×4 matrices of the following types, according to the relations between the two atoms to which the two atomic orbitals U_μ and U_ν belong: (i) the same atom – in this case, the 4×4 matrix is a unit matrix I; (ii) nearest neighbors; (iii) next nearest neighbors; (iv) different atoms separated by more than the next-nearest-neighbor distance – in this case, the overlap integrals are so small compared to those of the former three cases that we approximate these matrices by 4×4 zero matrices 0. A matrix of type (ii) (between atoms 1 and 2) and one of type (iii) (between atoms 1 and 3) are given in Table II.

The matrix (S_{ij}) can similarly be decomposed into 4×4 matrices. The diagonal blocks of 4×4 are again unit matrices. Because of the molecular symmetry there are only four different nonzero 4×4 matrices. Two of them, which we shall denote by S_{12} and S_{13}, are obtained from the two matrices $(S_{\mu\nu})$, given in Table II according to the transformation Eq. (23). The other two, which we shall denote by R_{12} and R_{13}, are obtained from S_{12} and S_{13} by interchanging the indexes 1 and 2 [which correspond to the hybrids a and b of Eqs. (15) and (16), respectively]. The 32×32 matrix (S_{ij}) can now be represented by the six 4×4 matrices I, S_{12}, S_{13}, R_{12}, R_{13}, and 0 as shown in Table III. Because of the symmetry of the matrix (S_{ij}) with respect to the diagonal, only the upper half is shown.

Now the normalization factor N_k can be calculated from Eq. (21). The results are given in the

TABLE II. Overlap integrals.

Basic overlap integrals

Distance (A)	$\langle 3s \mid 3s \rangle$	$\langle 3s \mid {}^3p\sigma \rangle$	$\langle 3p\sigma \mid 3p\sigma \rangle$	$\langle 3p\pi \mid 3p\pi \rangle$
2.048	0.1968	0.3230	0.3147	0.1897
3.312	0.0262	0.0742	0.1176	0.0350

Overlap integrals $(S_{\mu\nu})$ between atomic orbitals centered on atoms 1 and 2. The matrix is symmetric.

	s_2	ξ_2	η_2	ζ_2
s_1	0.1968	−0.1082	0.2612	−0.1563
ξ_1		0.1907	−0.0024	0.0817
η_1			0.1955	−0.1973
ζ_1				−0.0716

Overlap integrals $(S_{\mu\nu})$ between atomic orbitals centered on atoms 1 and 3. The matrix is symmetric.

	s_3	ξ_3	η_3	ζ_3
s_1	0.0262	−0.0525	−0.0525	0.0
ξ_1		0.0763	0.0413	0.0
η_1			0.0763	0.0
ζ_1				0.0350

Overlap integrals between hybrid orbitals centered on atoms 1 and 2, S_{12}. The matrix is symmetric.

	a_2	b_2	c_2	d_2
a_1	0.5609	0.0672	0.0713	0.0713
b_1		−0.0355	−0.1169	0.1037
c_1			0.0969	−0.0363
d_1				−0.1109

Overlap integrals between hybrid orbitals centered on atoms 1 and 3, S_{13}.

	a_3	b_3	c_3	d_3
a_1	−0.0043	0.1252	−0.0324	0.0452
b_1	0.0189	−0.0043	−0.0206	−0.0108
c_1	−0.0206	−0.0324	−0.0167	−0.0281
d_1	−0.0108	0.0452	−0.0281	0.0531

TABLE III. Overlap integral matrix S_{ij} (32×32) expressed in terms of the six 4×4 matrices 0, I, S_{12}, S_{13}, R_{12} and R_{13}. The matrix is symmetric with respect to the diagonal.

Atoms	1	2	3	4	5	6	7	8
1	I	S_{12}	S_{13}	0	0	0	R_{13}	R_{12}
2		I	R_{12}	R_{13}	0	0	0	S_{13}
3			I	S_{12}	S_{13}	0	0	0
4				I	R_{12}	R_{13}	0	0
5					I	S_{12}	S_{13}	0
6						I	R_{12}	R_{13}
7							I	S_{12}
8								I

last column of Table I.

The group overlap G_{kl} between two LCHO's ϕ_k and ϕ_l can be written in terms of S_{ij} and N as

$$G_{kl}=\langle \phi_k|\phi_l\rangle = N_k N_l \sum_{ij} f_{ki} f_{lj} S_{ij} \ . \tag{24}$$

The group overlaps between LCHO's, belonging to different irreducible representations, vanish by group-theoretical arguments. In Table IV, we present the group overlap matrices (G_{kl}) for each irreducible representation in which there are more than one LCHO.

V. SECULAR EQUATION

A MO ψ_m is represented as a linear combination of LCHO's ϕ_k,

$$\psi_m = \sum_k C_{mk} \phi_k \ . \tag{25}$$

The coefficients C_{mk} are determined by the solution of the secular equations

$$\sum_l (H_{kl} - G_{kl} E_m) C_{ml} = 0 \quad \text{for each } k, \tag{26}$$

where E_m is the energy of the MO ψ_m, G_{kl} is the group overlap matrix element (Table IV), and H_{kl} is the Hamiltonian matrix element between ϕ_k and ϕ_l.

Since there is no nonvanishing matrix elements of G and H between two LCHO's ϕ_k and ϕ_l, which belong to different irreducible representations, the secular equation [Eq. (26)] can be solved separately for each irreducible representation.

The Hamiltonian matrix element H_{kl} can be expanded in terms of matrix elements between two hybrid orbitals,

TABLE IV. Group overlap matrix elements between the LCHO's of Table I. The matrices are symmetric.

Ir. Rep.	Group overlap matrices		
A_1	1.0	−0.0939	0.2351
		1.0	−0.1235
			1.0
B_2	1.0	−0.0165	−0.2503
		1.0	0.0155
			1.0
E_1	1.0	0.5838	−0.1018
		1.0	0.1204
			1.0
E_2	1.0	−0.1772	−0.2143
		1.0	0.1936
			1.0
E_3	1.0	0.5373	−0.1905
		1.0	−0.1395
			1.0

				0.1578
				0.1094
				−0.0524
				1.0
				−0.0032
				−0.0558
				0.0604
				1.0
				0.0346
				0.2044
				0.0513
				1.0

TABLE V. Hamiltonian matrix elements between LCHO's of Table I. The matrices are symmetric.

Ir. Rep.	Hamiltonian matrix elements in eV			
A_1	−17.29	2.48	− 6.26	
		−16.43	3.41	
			−12.51	
A_2	− 7.04			
B_1	−13.23			
B_2	− 7.47	0.68	6.62	
		−11.67	− 0.42	
			−17.20	
E_1	−13.64	−11.98	2.64	− 4.15
		−15.92	− 3.19	− 2.99
			−15.58	1.45
				−11.73
E_2	− 4.69	4.61	5.58	0.18
		−16.26	− 5.16	1.46
			−13.57	− 1.67
				−12.47
E_3	−12.93	−10.18	5.07	− 0.94
		−11.89	3.63	− 5.44
			−12.04	− 1.42
				−15.75

$$H_{kl} = N_k N_l \sum_i \sum_j f_{ki} f_{lj} H_{ij} \ . \tag{27}$$

In the semiempirical MO calculations,[5] the diagonal elements H_{ii} are approximated by the valence-state ionization energies (VSIE) of the orbital i, and the off-diagonal elements H_{ij} $(i \neq j)$ are approximated by

$$H_{ij} = \tfrac{1}{2} F S_{ij} (H_{ii} + H_{jj}) \ . \tag{28}$$

Several different values (between 1 and 2) for the multiplicative factor F have been suggested by various authors. In this calculation we choose the value suggested by Cusachs[11]

$$F = 2 - |S_{ij}| \ . \tag{29}$$

We shall discuss the dependence of the final results on this factor in Sec. VII.

Ballhausen and Gray[12] have given the following values for the VSIE of sulfur 3s and 3p orbitals:

$$E_{3s} = -167 \times 10^3 \text{ cm}^{-1} = -20.70 \text{ eV} \ , \tag{30}$$

$$E_{3p} = -94 \times 10^3 \text{ cm}^{-1} = -11.65 \text{ eV} \ . \tag{31}$$

Thus, from Eqs. (1)–(4) and Eqs. (15)–(18), the VSIE of the σ hybrids a and b and the lone pairs c and d are, respectively,

$$H_{aa} = H_{bb} = \alpha^2 E_{3s} + (1-\alpha^2) E_{3p} = -13.78 \text{ eV} \ , \tag{32}$$

$$H_{cc} = H_{dd} = (0.5-\alpha^2) E_{3s} + (0.5+\alpha^2) E_{3p} = -14.05 \text{ eV} \ . \tag{33}$$

The matrix (H_{kl}) calculated from Eqs. (27)–(33)

TABLE VI. MO energies (in eV) and MO coefficients of S_8. The MO's are indexed in order of increasing energy.

Ir. Rep.	MO energy	MO coefficients				MO index
A_1	−18.53	−0.728	0.423	−0.310		1
	−15.78	+0.544	0.891	0.026		11
	−10.11	0.487	−0.220	−0.987		22
A_2	− 7.04	1				25
B_1	−13.23	1				16
B_2	−17.68	0.201	−0.036	−0.929		2
	−11.68	−0.049	0.997	−0.076		17
	− 5.08	1.012	0.068	0.445		26
E_1	−17.45	0.352	0.680	0.179	0.198	5, 6
	−16.26	−0.325	0.130	0.878	−0.194	9, 10
	−10.64	−0.129	−0.283	0.243	0.967	20, 21
	− 3.98	1.167	−1.019	0.450	−0.123	27, 28
E_2	−17.52	−0.151	0.779	0.417	−0.021	3, 4
	−13.45	−0.084	−0.365	0.537	0.748	14, 15
	−10.69	−0.116	−0.543	0.688	−0.670	18, 19
	− 2.02	1.013	0.173	0.383	−0.018	31, 32
E_3	−16.81	0.233	0.384	−0.109	0.741	7, 8
	−15.29	−0.504	−0.155	0.510	0.531	12, 13
	− 9.22	0.476	0.257	0.879	−0.312	23, 24
	− 3.21	0.953	−1.116	0.028	0.360	29, 30

are given in Table V. The solutions of the secular equation [Eq. (26)], i.e., the MO energies E_m and the MO coefficients C_{mk}, are given in Table VI. The MO's are indexed in order of increasing energy. Since there are $6\times8=48$ valence electrons in a S_8 molecule, the lower 24 MO's are occupied. The energy-level diagram is shown in Fig. 2.

VI. ELECTRONIC TRANSITIONS

The three-dimensional vector representation reduces into the irreducible representations $B_2(z)$ and $E_1(x,y)$ in the point group D_{4d}. The selection rule for electric dipole transitions derived from the character table is shown in Table VII. The ∥ and ⊥ signs indicate that the transitions between the two levels are allowed for the polarization, parallel and perpendicular, respectively, to the

TABLE VII. Selection rule for electronic dipole transitions in S_8. The ∥ and ⊥ signs denote allowed transitions with polarization parallel and perpendicular, respectively, to the molecular z axis (Fig. 1); 0 denotes forbidden transitions.

	A_1	A_2	B_1	B_2	E_1	E_2	E_3
A_1	0	0	0	∥	⊥	0	0
A_2	0	0	∥	0	⊥	0	0
B_1	0	∥	0	0	0	0	⊥
B_2	∥	0	0	0	0	0	⊥
E_1	⊥	⊥	0	0	0	⊥	∥
E_2	0	0	0	0	⊥	∥	⊥
E_3	0	0	⊥	⊥	∥	⊥	0

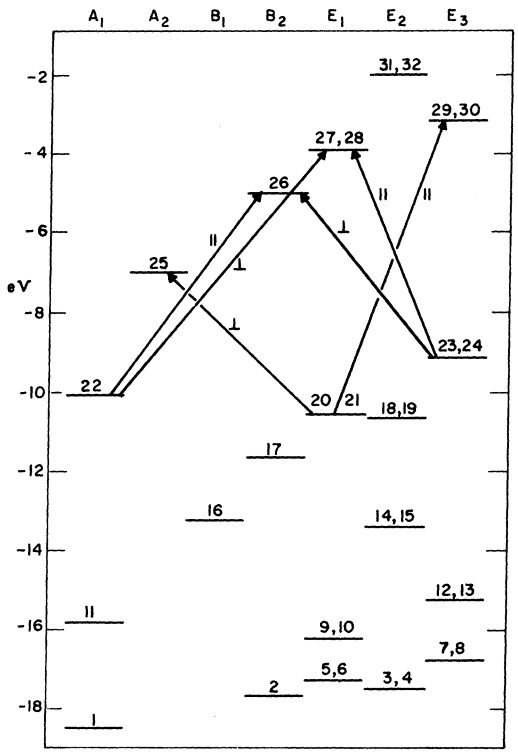

FIG. 2. MO energy levels of S_8. Levels of the same irreducible representation (which is given in the top line) are shown in the same column. MO indexes are given with the levels. Doubly degenerate levels carry two indexes. Several allowed electronic transitions with their polarizations are shown by arrows.

molecular z axis (which is perpendicular to the molecular planes). Several lower-energy transitions with their polarizations are also shown in Fig. 2.

As mentioned in the Introduction, there are no detailed spectroscopic data to compare with this prediction. From the spectrum published by Baer and Carmack,[4] it is possible to resolve three peaks at 4.4, 4.8, and 5.4 eV. These three peaks could be assigned to the following transitions, respectively:

$$E_1\ (\text{MO}\,20, 21) \rightarrow A_2(25), \quad \Delta E(\text{calc}) = 3.6\ \text{eV}\ ,$$

$$E_3\ (\text{MO}\,23, 24) \rightarrow B_2(26), \quad \Delta E(\text{calc}) = 4.1\ \text{eV}\ ,$$

$$A_1\ (\text{MO}\,22) \rightarrow B_2(26), \quad \Delta E(\text{calc}) = 5.0\ \text{eV}\ .$$

There are no polarization data to support the assignment. The differences between the observed transition energies and ΔE(calc) could be attributed to the electron correlation in the final states. We shall not pursue this matter further here.

A more important result in this analysis is that the two lowest-energy transitions

$$E_3\ (\text{MO}\,23, 24) \rightarrow A_2\ (25), \quad \Delta E(\text{calc}) = 2.2\ \text{eV}\ ,$$

$$A_1\ (\text{MO}\,22) \rightarrow A_2\ (25), \quad \Delta E(\text{calc}) = 3.1\ \text{eV}$$

are symmetry forbidden. These transitions, however, become allowed when S_8 molecules are packed into orthorhombic crystals or when changes in molecular vibrational states accompany the transitions. This could be the origin of the yellow color of sulfur crystals and the long tail extending below 3 eV in the solution spectra of sulfur.[4]

In the following paper[13] we also present an argument that one of these transitions $A_1 \rightarrow A_2$ may be responsible for the nonphotoconducting absorption.

VII. DISCUSSION

First, we like to point out that there is considerable overlap between the σ hybrids and the lone-pair hybrids, as can be seen from Table II (S_{12} and S_{13}). In fact the overlap between the hybrids b and c (or d) on nearest-neighbor atoms is as large as the overlap between two c (or d) hybrids. Consequently, in most MO's, all four kinds of hybrids coexist. For example, in the highest occupied MO (23 and 24), the fraction of σ hybrids is about 30% (see Table VI), whereas in Gibbons and Spear's model,[1,3] this MO consists of only lone-pair hybrids. The only exceptions are MO 16 (B_1) and MO 25 (A_2). Since the lone-pair hybrids do not form combinations transforming as B_1 or A_2, these two MO's consist only of σ hybrids. The MO 25 (A_2) is the lowest empty orbital which is expected to form the excess electron band in orthorhombic sulfur crystals. Since the σ hybrids are more concentrated within the molecule, the intermolecular overlap between two such orbitals is expected to be small. This argument has been used by Spear and co-workers[1] to explain the experimental findings that an excess electron moves by a hopping process, while an excess hole propagates in a polaron band in orthorhombic sulfur.

An examination of the energy-level diagram (Fig. 2) shows that the two lowest empty orbitals, MO 25 and MO 26, are separated by about 2 eV, whereas in the upper occupied orbitals, there are seven MO's (MO 18–MO 24) within the range of 2 eV. The close lying of these levels may allow the energy bands generated from these MO's to overlap, resulting in a wider band for the hole transport.

Perhaps the largest uncertainty in this calculation is the choice of the multiplication factor F in Eq. (28). The choice of Eq. (29) corresponds to using a smaller value of F for orbitals with larger overlaps. This is consistent with the practice[5] of using a smaller value (1.6) for σ bonds and a larger value (1.87) for π bonds.

Calculations using a constant value for F (varying from 1.25 to 2.0) show that the resulting MO energies vary quite drastically. For example, the separation between the highest occupied and the lowest empty MO levels varies from 3.2 to 12.3 eV. It seems that the energy levels obtained with Eq. (29) are in the best accord with the optical data,[4] although there could be uncertainties as large as ± 0.5 eV.

On the other hand, the above-mentioned fact (that there are seven occupied MO levels within the energy range equal to the separation between the two lowest empty levels) always holds true, although the energy range varies from 0.4 to 1.7 eV.

It is also found from these calculations that the MO coefficients, C_{mi} are very weakly dependent on the value of F. All coefficients vary less than 10% (many of them vary less than 3%) in the range $1.25 \leq F \leq 2.0$. The differences between the coefficients obtained by using Eq. (29), and those obtained by using a constant F, are slightly larger, but very seldom exceed 0.1 in absolute value. Since in the calculations of intermolecular integrals (see following paper[13]) the larger coefficients dominate the results, an absolute error of 0.1 in quantities of the order of 1 is tolerable in comparison to other approximations made in the calculation.

Thus we conclude that the MO's we obtained in this calculation (Table VI) are sufficiently good to use as a basis for describing the electronic states of orthorhombic sulfur crystals (see the following paper).

[1]A. R. Adams and W. E. Spear, J. Phys. Chem. Solids 25, 1113 (1964); W. E. Spear and A. R. Adams, *ibid.* 27, 281 (1966); D. J. Gibbons and W. E. Spear, *ibid.* 27, 1917 (1966); P. K. Ghosh and W. E. Spear, J. Phys. C. 1, 1347 (1968); B. E. Cook and W. E. Spear, J. Phys. Chem Solids 30, 1125 (1969).
[2]S. A. Rice and J. Jortner, in *Physics of Solids at High Pressures*, edited by C. T. Tomizuka and R. M. Emrick (Academic, New York, 1965), p. 63.
[3]D. J. Gibbons (unpublished), report supplied by Professor W. E. Spear.
[4]J. E. Baer and M. Carmack, J. Am. Chem. Soc. 71, 1215 (1949).
[5]M. Wolfsberg and L. Helmholz, J. Chem. Phys. 20, 837 (1952).
[6]S. C. Abrahams, Acta Cryst. 8, 661 (1955); A. Caron and J. Donohue, *ibid.* 14, 548 (1961).
[7]G. Herzberg, *Molecular Spectra and Molecular Structure* (Van Nostrand, Princeton, N.J., 1966), Vol. III, p. 566.
[8]C. J. Ballhausen, *Introduction to Ligand Field Theory* (McGraw-Hill, New York, 1962), Chap. 7.
[9]R. S. Mulliken, C. A. Rieke, D. Orloff, and H. Orloff, J. Chem. Phys. 17, 1248 (1949).
[10]R. E. Watson and A. J. Freeman, Phys. Rev. 123, 521 (1961).
[11]L. C. Cusachs, J. Chem. Phys. Suppl. 43, 157 (1965); L. C. Cusachs and J. W. Reynolds, *ibid.* 43, 160 (1965).
[12]C. J. Ballhausen and H. B. Gray, *Molecular Orbital Theory* (Benjamin, New York, 1964), p. 122.
[13]I. Chen, following paper, Phys. Rev. B 2, 1060 (1970).

PHYSICAL REVIEW B VOLUME 2, NUMBER 4 15 AUGUST 1970

Molecular-Orbital Studies of Charge-Carrier Transport in Orthorhombic Sulfur. II. Electronic States of the Crystal

Inan Chen
Research Laboratories, Xerox Corporation, Rochester, New York 14603
(Received 16 January 1970)

In order to interpret the difference of four orders of magnitude in the electron and the hole drift mobilities in orthorhombic sulfur, the intermolecular electronic-interaction energies for an excess electron and an excess hole are computed with the molecular orbitals obtained in the preceding paper. The excess-carrier energy bands are obtained by summing these energy integrals according to the symmetry characteristics of the crystal structure. Contrary to what Spear and co-workers have expected, the electronic contributions to the widths of an excess electron band and an excess hole band are found to be of the same order of magnitude and hence do not account for the large difference in the mobilities. The changes in the electronic charge distributions when an electron is added to or removed from a neutral molecule are used to estimate the relative values of molecular deformations and the polaron binding energies E_b. It is found that E_b associated with an excess electron is almost an order of magnitude larger than that associated with an excess hole. Holstein and Siebrand's theory is then used to show that this difference in electron-molecular vibration couplings is the major effect leading to the large difference in the electron and the hole mobilities. The same argument is used to explain the large difference in the charge-carrier mobilities of metal-free phthalocyanine and copper phthalocyanine. The excitation-transfer matrix elements are formulated in terms of molecular-orbital coefficients. The matrix elements for one of the excited states are found to be always almost zero due to the molecular symmetry. This is interpreted as the "localized excited state" which is responsible for the nonphotoconducting absorption observed in orthorhombic sulfur and vitreous selenium.

I. INTRODUCTION

In the preceding paper, [1] we have already mentioned the experimental works of Spear and co-workers[2] on the electric and optical properties of orthorhombic sulfur. The crystal of orthorhombic sulfur consists of S_8 molecules held together by van der Waals forces. It is therefore possible to study the electronic states of the crystal from those of an isolated S_8 molecule by treating the intermolecular interaction as a perturbation.[3]

With 16 molecules in a unit cell, the crystal structure of orthorhombic sulfur is considerably more complicated than those of well-studied organic molecular crystals such as naphthalene or anthracene. The crystal structure and the space group are analyzed in detail, and the symmetry-adapted-crystal wave functions are derived in Sec.